Localization-dependent activity of the Kv2.1 delayed-rectifier K⁺ channel

Kristen M. S. O'Connell[a,1], Robert Loftus[a], and Michael M. Tamkun[a,b,2]

Departments of [a]Biomedical Sciences and [b]Biochemistry and Molecular Biology, Colorado State University, Fort Collins, CO 80523

The Kv2.1 K⁺ channel is highly expressed throughout the brain, where it regulates excitability during periods of high-frequency stimulation. Kv2.1 is unique among Kv channels in that it targets to large surface clusters on the neuronal soma and proximal dendrites. These clusters also form in transfected HEK cells. Following excessive excitatory stimulation, Kv2.1 declusters with an accompanying 20- to 30-mV hyperpolarizing shift in the activation threshold. Although most Kv2.1 channels are clustered, there is a pool of Kv2.1 resident outside of these domains. Using the cell-attached patch clamp technique, we investigated the hypothesis that Kv2.1 activity varies as a function of cell surface location. We found that clustered Kv2.1 channels do not efficiently conduct K⁺, whereas the nonclustered channels are responsible for the high threshold delayed rectifier K⁺ current typical of Kv2.1. Comparison of gating and ionic currents indicates only 2% of the surface channels conduct, suggesting that the clustered channels still respond to membrane potential changes. Declustering induced via either actin depolymerization or alkaline phosphatase treatment did not increase whole-cell currents. Dephosphorylation resulted in a 25-mV hyperpolarizing shift, whereas actin depolymerization did not alter the activation midpoint. Taken together, these data demonstrate that clusters do not contain high threshold Kv2.1 channels whose voltage sensitivity shifts upon declustering; nor are they a reservoir of nonconducting channels that are activated upon release. On the basis of these findings, we propose unique roles for the clustered Kv2.1 that are independent of K⁺ conductance.

actin depolymerization | gating currents | Kv2.1 clustering | single-channel activity | confocal imaging

Voltage-gated K⁺ channels (Kv channels) are a diverse family of K⁺-selective ion channels that play a critical role in the regulation of excitability in many cell types. Kv channels are responsible for establishment of the resting membrane potential, repolarization during action potentials, and regulation of action potential frequency (1). Most cells express multiple isoforms of Kv channels, some of which are functionally similar (e.g., the A-type channels Kv1.4 and Kv4.2), but exhibit a striking specificity to their subcellular localization (e.g., Kv4.2 is expressed in distal dendrites, whereas Kv1.4 is axonal) (2). Thus, the localization of Kv channels may be an important determinant in their role in modulating cellular excitability.

The delayed rectifier Kv2.1 channel is expressed in a variety of cell types: It regulates spike frequency in neurons (3), is a key component of repolarization in rat cardiac myocytes (1), and regulates insulin secretion in pancreatic β cells (4). It is perhaps best characterized in mammalian neurons, where it underlies a majority of the somato-dendritic delayed rectifier K⁺ current (5). Relative to other Kv channels, Kv2.1 exhibits a high threshold for activation ($+10$–20 mV activation midpoint) and primarily regulates excitability during periods of high-frequency firing in pyramidal cells (3, 6) or tonic firing in sympathetic neurons (7). The threshold for activation of Kv2.1 is shifted to more negative potentials in response to various excitatory stimuli (e.g., glutamate, ischemia, muscarinic activation, elevated cytoplasmic Ca^{2+}); it is presumably via this mechanism that Kv2.1 selectively regulates neuronal excitability during periods of high-frequency excitotoxic

stimuli (8–10). Kv2.1 also plays a well-established role in apoptosis (11), where it may mediate the KCl loss involved in cell death.

One of the hallmarks of Kv2.1 expression in mammalian neurons is specific targeting to large, high-density cell surface clusters restricted to the soma and proximal dendrites (8, 12, 13). Interestingly, not only is channel voltage dependence altered by the aforementioned stimuli, but also channel localization. In response to the aforementioned stimuli, the Kv2.1 cluster pattern changes to a more diffuse localization (8, 9), suggesting a close relationship between channel function and channel localization. Channel dephosphorylation occurs in parallel with this declustering and the hyperpolarizing shift in activation midpoint (8, 10). These findings have led to the untested general hypothesis that clustered channels are phosphorylated and thus have a high threshold for activation whereas the nonclustered, or experimentally declustered, channels are dephosphorylated and generate low-threshold currents.

Although the majority of Kv2.1 channels reside within the cell surface clusters, at steady state there is a small pool of channels outside this domain (14). In this study, we examined Kv2.1 channel activity as a function of cell surface location using the cell-attached patch clamp technique with confocal imaging. Although clustered Kv2.1 channels are responsive to changes in membrane potential based on gating current measurements, they do not conduct K⁺. In contrast, the nonclustered channels are responsible for the high-threshold delayed rectifier currents attributed to Kv2.1. This result in turn led to the hypothesis that the Kv2.1 clusters represent cell surface storage sites containing nonfunctional channels that are then activated upon declustering. However, two functionally distinct declustering stimuli failed to increase whole-cell currents. On the basis of these findings, we propose unique roles for the clustered Kv2.1 that are independent of K⁺ conductance.

Results

Clustered Kv2.1 Channels Do Not Readily Conduct Potassium. Primary cell culture model systems such as embryonic hippocampal neurons express a large complement of endogenous ion channels, including multiple voltage-gated K⁺ channels, making the assignment of currents from cell-attached patches to a specific channel difficult, if not impossible. For these experiments, a high degree of confidence in the identity of the ion channel was critical, thus necessitating the use of a model system such as HEK cells with a null background. Kv2.1 is expressed well in HEK293 cells and targets to cell surface clusters similar to those found in neurons. In addition, Kv2.1 function and localization in

NEUROSCIENCE

HEK293 cells are regulated by the same stimuli that modulate channel function in neurons (15). Because low passage HEK293 cells express few endogenous ion channels (we recorded no endogenous channel activity in nontransfected controls), we chose this system for the experiments in this study. We previously generated a tagged Kv2.1 construct, GFP-Kv2.1loopBAD (13, 14) that carries green fluorescent protein (GFP) on the N terminus of Kv2.1 and a biotin acceptor domain (BAD) within the extracellular S1–S2 loop, enabling specific labeling of cell surface channels with streptavidin-conjugated quantum dots as illustrated in Fig. S1. This construct is functionally identical to wild-type Kv2.1, even with bound streptavidin-conjugated quantum dots (Qdots), as shown in Fig. S2. This construct, but without the bound Qdots, was used for all of the experiments summarized in Figs. 1–4 below.

As previously described, Kv2.1 clusters are high-density structures containing most of the Kv2.1 expressed on the plasma membrane (8, 13, 14). Binding of various reagents to extracellular epitopes has confirmed that these structures are indeed on the cell surface (13). We hypothesized that the channels associated with these structures underlie the large high-threshold K$^+$ current attributed to Kv2.1 under steady-state conditions. To test this, we took advantage of the size of these clusters (~2 μm in diameter) and used cell-attached patch clamp to measure channel activity in these domains. The use of high-magnification confocal microscopy and the GFP tag on Kv2.1 allowed us to
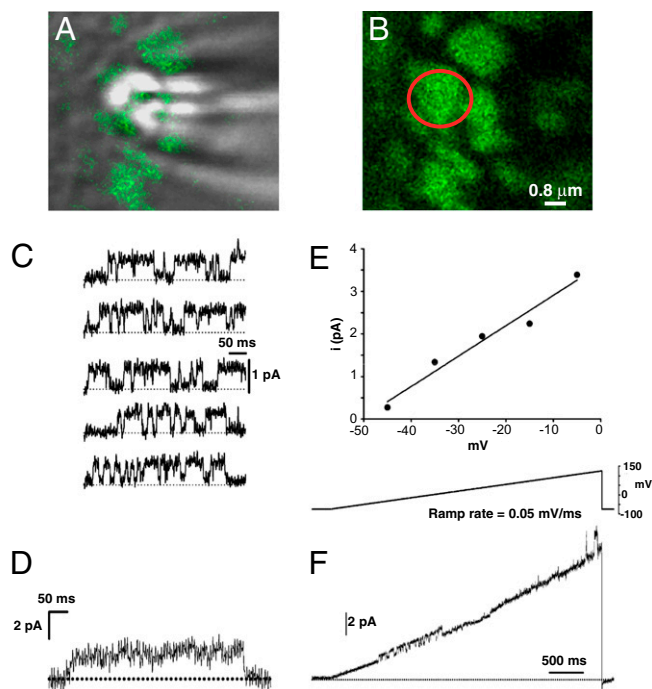
Fig. 1. Kv2.1 channels retained within cell surface clusters are nonconducting. (A) Overlay of the GFP fluorescence (green) and DIC images of the apical surface of a GFP-Kv2.1-loopBAD-expressing HEK cell during an on-cluster cell-attached patch-clamp experiment. The white spots are due to diffracted light from the patch pipette. (B) Fluorescence only image of the GFP-Kv2.1-loopBAD cluster targeted for cell-attached patch clamp. The red circle indicates the position of the patch pipette. (C) Representative sweeps at −15 mV from the cell in A. Upward deflections indicate channel opening, dashed line is zero current. (D) Ensemble average of 71 sweeps containing Kv2.1 channel activity. (E) Current–voltage relationship for all cell-attached on-cluster patches, n = 32. Data for each point are derived from a Gaussian fit to an all-points histogram of the total dataset at each potential. Error bars are smaller than the symbols. The slope conductance is 7.1 pS. (F) Ramp depolarization of an on-cluster patch from −75 to +125 mV at 0.05 mV/ms. Channel activity (upward deflection) is observed between −30 and +5 mV and again at +120 mV.

accurately position the patch pipette onto these clusters as shown in Fig. 1A. To measure channel activity, the patch illustrated in Fig. 1B was depolarized from the resting membrane potential (RMP) (−75 mV) to test potentials from −45 mV to −5 mV for 400 ms. Representative leak-subtracted sweeps from depolarizations to −15 mV are shown in Fig. 1C. Upward deflections represent channel opening. Despite strong GFP fluorescence beneath the patch pipette (Fig. 1B), there was very little channel activity in any of the on-cluster patches. This particular on-cluster patch contained only one active channel. Shown in Fig. 1D is the ensemble current from 77 sweeps to −15 mV, which exhibits the slow activation kinetics typical of macroscopic Kv2.1 current. The unitary conductance of this channel as determined from the slope conductance illustrated in Fig. 1E was 7.1 pS, in good agreement with previous estimates for Kv2.1 (16, 17). Rarely, multiple channels were active in an on-cluster patch and we never observed more than three active channels in a single patch (2 patches had two channels and only 1 had three). Furthermore, no channel activity was observed in 18 of 32 on-cluster patches (53%), with a low amount of single-channel activity detected in the remaining 14 patches.

One possible explanation for the minimal channel activity observed within the clusters was that the test depolarizations were insufficient to activate Kv2.1, particularly considering the high threshold for Kv2.1 activation (our maximal V_{test} was +5 mV). Therefore, to better evaluate the voltage dependence of the clustered Kv2.1 channels, we used a ramp protocol to depolarize on-cluster patches from the resting membrane potential of −75 mV to a maximal final potential of +125 mV. If the low level of channel activity observed in the on-cluster patches was due to insufficiently strong depolarization, channel activity should increase dramatically as membrane potential gradually depolarizes during the ramp. However, as shown in Fig. 1F, this was not the case. A burst of channel activity from a single channel was seen between −30 and +5 mV (the range we used for the episodic recordings), but even at ~ +120 mV, only single-channel activity was observed. This result suggests that Kv2.1 channels retained with cell-surface clusters are truly nonconducting K$^+$ channels and do not contribute significantly to the macroscopic delayed rectifier K$^+$ current. Taken together, these on-cluster single-channel data strongly suggest that the channel recorded in these patches is Kv2.1.

Robust Kv2.1 Current Is Obtained from Off-Cluster Cell-Attached Patches. Using streptavidin-Qdot labeling of extracellular S1–S2 loop biotinylated Kv2.1 (14), we readily detected nonclustered Kv2.1 channels on the cell surface of HEK293 cells exhibiting robust (>10 nA) delayed rectifier currents (Figs. S1 and S2). The results presented in Fig. 1 raise the possibility that nonclustered channels are responsible for the macroscopic delayed rectifier current. Therefore, we used the cell-attached patch clamp technique to measure the activity of nonclustered channels under identical conditions to those used to measure clustered channel activity.

For these experiments, the patch pipette was carefully positioned on regions of the plasma membrane devoid of Kv2.1 clusters (Fig. 2A). The patches were depolarized from the RMP to test potentials from −135 mV to +60 mV for 200 ms; representative sweeps are shown in Fig. 2B. In striking contrast to the on-cluster patches, off-cluster patches exhibited robust delayed rectifier currents with slow activation kinetics typical of Kv2.1. At +60 mV (where channel activation is maximal), using a value of 0.96 pA as the single-channel current and assuming $P_o = 0.7$ (18, 19), at least 250 Kv2.1 channels are required to generate the currents seen in Fig. 2B. Most of the off-cluster patches had currents >1 nA (7 of 11). Patches with this current magnitude were unstable, with either high-resistance seals being lost or the patch rupturing entirely. The current–voltage relationship for the off-cluster currents was measured from 4 patches with currents <300 pA (Fig. 2C). The acti-

vation midpoint obtained from the conductance–voltage relationship of the off-cluster patches was nearly identical to that of the macroscopic $I_{Kv2.1}$, $+10.6 \pm 3.6$ mV, $n = 4$ (Fig. 2D) vs. $+6.7 \pm 6.8$ mV, $n = 6$, for whole-cell $I_{Kv2.1}$ (Fig. 2D, red curve, and Fig. S2). Taken together, the results illustrated in Figs. 1 and 2 strongly suggest that the nonclustered Kv2.1 channels are responsible for most of the whole-cell Kv2.1 delayed rectifier current.

Clustered Kv2.1 Channels Sense Changes in Membrane Potential. The extreme functional differences between the on- and off-cluster channels led us to question whether the clustered, nonconducting Kv2.1 channels were still responsive to changes in membrane potential. As with all voltage-gated ion channels, the S4 domain of the Kv2.1 α-subunit contains a series of positively charged residues that contribute to the voltage-sensing capability of the channel. Movement of these intramembranous charges in response to changes in membrane potential results in a measureable gating current (20). Because movement of these gating charges occurs before and independently of opening of the ion-conducting pore, a surface channel with a functional voltage sensor generates gating currents, regardless of its ion conduction properties.

Ideally, measurement of the gating currents from clustered Kv2.1 channels would be done using on-cell patch clamp of these domains. However, gating currents are extremely small (< 20 fA per channel) and are readily masked by ionic current. Because intracellular K^+ is present in the cell-attached configuration, ionic current contamination is likely. In addition, the RMS noise
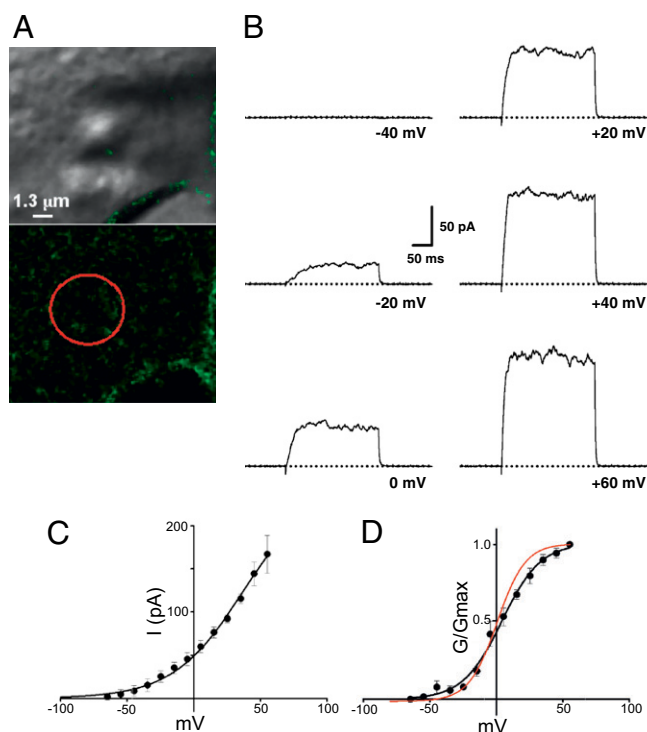
Fig. 2. Nonclustered Kv2.1 channels are conducting K^+ channels. (A) DIC and GFP fluorescence images of the apical surface of a GFP-Kv2.1-loopBAD-expressing HEK cell. The red circle in the GFP fluorescence image shows the location of the patch pipette, demonstrating there are no Kv2.1 clusters near the patch pipette. (The scale bar applies to both micrographs.) (B) Representative sweeps to the indicated potentials from an off-cluster patch. (C) Current–voltage relationship from four off-cluster patches. (D) Conductance–voltage relationship calculated from the data in C, assuming an intracellular [K^+] of 140 mM and thus a reversal potential of −84 mV. $V_{1/2}$ of the fitted data from conductance–voltage plot = +10.6 mV. The red plot illustrates the voltage dependence as obtained from whole-cell currents illustrated in Fig. S2.

in our patch clamp system complicates the detection of gating current arising from a small number of Kv2.1 channels. Therefore, we measured the total macroscopic gating charge and compared it to the macroscopic I_K. To accurately measure gating currents, the ionic current was eliminated using 130 mM extracellular tetraethylammonium (TEA) to block the Kv2.1 pore and substitution of internal K^+ with 140 mM $NMDG^+$. Gating currents were then measured using whole-cell voltage clamp from test potentials from −80 mV to +80 mV, using 200-ms pulses as illustrated in Fig. 3A. All traces were leak and capacitance subtracted and the total gating charge moved was measured by integration of the initial transient current ("Q_{on}") produced following membrane depolarization (Fig. 3A Inset). Fig. 3B compares the voltage dependence of the gating current to that of the ionic current in Fig. S2. The midpoint of activation for the Kv2.1 Q–V curve is > −30 mV shifted from that of the G–V curve ($V_{Q1/2} = -27.0 \pm 4.0$ mV, $n = 8$) (Fig. 3C). Whereas it is common for the gating current voltage dependence of channels to be shifted in the hyperpolarizing direction relative to the ionic current (21, 22), a −30-mV shift is unusual. With such a large shift, the Kv2.1 voltage sensor is capable of detecting changes in membrane potential over a physiological range that is well below the threshold for activation of the K^+ current, raising the possibility that Kv2.1 may function as a voltage sensor to monitor neuronal activity.

To estimate channel number from gating current measurements, we used the value of Q_{on} at +60 mV, a potential at which channel activation is maximal. In these experiments, the mean Q_{on} at +60 mV was 2.3 ± 0.6 nC ($n = 8$). Using a previous measurement of 12.5 q_e per Kv2.1 gating cycle (19), we estimated the channel density in a Kv2.1-expressing HEK cell to be ≈600 channels/μm^2 (~1 × 10^6 channels per cell). We then estimated the number of Kv2.1 channels that underlie the delayed rectifier K^+ current in transfected HEK cells expressing similar levels of GFP-Kv2.1, using the peak macroscopic $I_{Kv2.1}$ at +60 mV according to the relationship $I = i \times N \times P_o$, where I is the peak K^+ current, i is the single-channel current at +60 mV, N is channel number, and P_o is open channel probability. In GFP-Kv2.1-expressing HEK cells, the peak $I_{Kv2.1} = 19.3 \pm 2.6$ nA ($n = 6$) and $i = 0.96$ (at +60 mV). Assuming $P_o = 0.7$ at +60 mV (19), ≈28,000 channels are required to generate a 19-nA current, for a channel density of ~14 channels/μm^2. This discrepancy is consistent with our finding that clustered Kv2.1 channels are nonconducting and suggests that despite not conducting K^+, these "silent" channels have S4 domains that move in response to changes in membrane potential.

Kv2.1 Channels Do Not Conduct K^+ Upon Declustering. Previous work using cultured hippocampal neurons suggests that declustering stimuli, while inducing a depolarizing shift in the voltage dependence of activation, do not increase whole-cell delayed rectifier current (9, 15), although a recent study (6) indicates that treatment of cultured hippocampal neurons with 10 μM glutamate for 10 min may cause a modest increase in the delayed rectifier current in these cells. However, these studies compared populations of cells and changes in whole-cell current amplitudes could have been missed due to cell-to-cell variability. To more directly address the possibility that the surface clusters might act as surface reservoirs of nonconducting channels that are then activated upon declustering, we performed simultaneous confocal imaging and whole voltage clamp before and after declustering. In this manner we were able to directly compare changes in current density to channel clustering.

We have previously shown that cortical actin is required to keep Kv2.1 within the cluster because actin depolymerization, with agents such as swinholide A, causes declustering (14). Therefore, our first experiment here was to depolymerize actin with swinholide A during whole-cell voltage clamp. Thus, the cell serves as its own control and the affect of declustering on both current magnitude

NEUROSCIENCE

Fig. 3. Nonconducting Kv2.1 channels on the cell surface respond to changes in membrane potential. (*A*) Representative gating currents at the indicated potentials for a GFP-Kv2.1-loopBAD-expressing HEK cell. (Scale bars: 1 nA, 50 ms.) (*Inset*) "On" gating current at +60 mV. (Scale bars: 1 pA, 2 ms.) (*B*) Normalized charge–voltage (*Q–V*) curve for GFP-Kv2.1-loopBAD. Q_{max} = 2.269 ± 571 nC, $V_{1/2}$ = −27.0 ± 4.0 mV (n = 8, $P < 0.01$, compared with $V_{G1/2}$). A fit to a single Boltzmann is shown because a fit of two distributions was not better. Red line is the fit from the conductance–voltage plot in Fig. S2B. (*C*) Scatter plot of the estimate of channel number from gating currents or ionic currents. The red line is the mean for each group. A value of 12.5 q_e per Kv2.1 channel was used to estimate channel number. $P < 0.01$.

and voltage sensitivity is readily monitored. As illustrated in Fig. 4*A*, a cell with obvious clusters was chosen for whole-cell voltage clamp and 200 nM swinholide A was added several minutes after control traces were obtained. After 25 min the channels had clearly declustered. Interestingly, we also saw a decrease in whole-cell current (16.2 vs. 10.3 nA, Fig. 4*C*) and membrane capacitance (14.9 pF vs. 13.4 pF). Thus, current density decreased from 1.08 to 0.77 nA/pF. Deactivation kinetics at −40 mV did slow upon declustering in only two of the six cells treated with swinholide A. Overall, swinholide A-induced declustering resulted in no change in current density (0.97 ± 0.15-fold decrease) or voltage dependence (−0.28 ± 4.0 mV shift in activation midpoint) in the six cells that could be maintained with satisfactory whole-cell properties during actin depolymerization. Thus, we conclude that actin depolymerization-induced declustering of Kv2.1 from the surface clusters does not result in activation of previously silent channels nor does it alter channel voltage dependence.

Physiological stimuli that mediate Kv2.1 declustering and increased voltage sensitivity in neurons (8, 9) and HEK cells (15)

involve calcineurin-mediated dephosphorylation. Therefore, we induced declustering via alkaline phosphatase in the patch clamp pipette. Again, cells with obvious clusters were imaged before and during the phosphatase dialysis and voltage clamp. Representative results are illustrated in Fig. 4 *D–F*. Comparison of the images in Fig. 4 *D* and *E* shows declustering over 15 min whereas Fig. 4*F* shows no change in steady-state current magnitude. However, current density in this cell did increase 1.16-fold. As previously reported, there was also a hyperpolarizing, or leftward, shift in the activation midpoint (activation midpoint = −9.6 mV after phosphatase treatment as compared with 2.1 mV before dephosphorylation) (15). The effect of alkaline phosphatase on inactivation kinetics was observed in three of the five cells that lasted long enough on the patch clamp pipette for declustering to be observed. Overall, there was no change (0.98 ± 0.13-fold) in current density and a 25.3 ± 2.6-mV depolarizing shift in the activation midpoint following phosphatase-induced declustering, n = 5. In summary, neither declustering maneuver activated a significant percentage of the nonconducting channels

Fig. 4. Kv2.1 declustering does not increase whole-cell current. GFP-Kv2.1-loopBAD-expressing HEK cells were imaged for GFP before and during whole-cell voltage clamp. (*A*) Cell with prominent surface clusters before whole-cell voltage clamp and actin depolymerization. (*B*) The same cell 25 min after the addition of 200 nM swinholide A. (*C*) Outward currents observed at +60 mV before and after swinholide A-induced declustering. (*D*) Cell with prominent surface clusters before alkaline phosphatase dialysis (500 units/mL in the intracellular pipette solution) and whole-cell voltage clamp. (*E*) The same cell 15 min after membrane rupture. (*F*) Outward currents observed at +60 mV before (1 min after break-in) and after phosphatase-induced declustering (after 15 min of whole-cell dialysis).

that represent 98% of the cell surface Kv2.1 on the basis of our gating current measurements. Because channel voltage dependence was affected by only the alkaline phosphatase-induced dephosphorylation, and not actin depolymerization, it is likely clustering and voltage sensitivity are independently regulated.

Discussion

This study examines the relationship between Kv2.1 function and localization in transfected HEK cells. It is noteworthy that the Kv2.1 expression levels and localization and the regulation of localization and function are nearly identical between transfected HEK cells and the endogenous Kv2.1 in cultured hippocampal neurons (8, 9, 13–15). We report here that the clustered Kv2.1 is nonconducting and that the majority of the whole-cell current is derived from the nonclustered channels. Furthermore, gating current measurements indicate that only 2% of the surface channels are conducting at +60 mV, suggesting that the clustered but nonconducting channels still respond to voltage.

Previous dogma based on elegant work by the Trimmer group (8–10) suggested that the clustered Kv2.1 channels have an activation midpoint of ∼ +15 mV and that upon declustering this value shifts to −20 mV. Because this change in voltage sensitivity and localization is paralleled by channel dephosphorylation (8–10), and voltage dependence is known to be regulated by multiple C-terminal phosphorylation sites (23), models that colocalize Kv2.1 with kinases in the cluster to maintain the highly phosphorylated, high-threshold state have been popular. These models (24) suggest that upon cluster release, phosphatases such as calcineurin then dephosphorylate the channel, thereby enhancing the voltage sensitivity. However, our results argue against such a model because not only are most of the clustered channels nonconducting, but also the nonclustered channels are high-threshold as opposed to low-threshold delayed rectifiers.

Upon first discovering that the clustered channels were nonconducting, we hypothesized that they could represent a cell surface reservoir where channels are stored until needed. This reservoir would provide the cell with a mechanism to rapidly up-regulate functional channel number on the cell surface without having to synthesize channels de novo and transport them to the surface. Because the declustering stimuli are often associated with neuronal injury, it was logical to propose that declustering might be associated with a dramatic increase in delayed rectifier magnitude, especially in the presence of a hyperpolarizing shift in the voltage dependence of activation. However, the data presented in Fig. 4 indicate that two distinct declustering stimuli, actin depolymerization and dephosphorylation, do not increase channel activity, although it is possible we have not used the optimal stimulus or that HEK cells do not fully mimic the in situ regulation. One interesting area for future research will be to examine the effect of apoptotic stimuli on Kv2.1 activation because this channel is essential for this oxidant-induced cell death (11, 25). Additional declustering stimuli will include N_2 saturated solutions as a means of establishing hypoxia (26). Ultimately, these declustering experiments will have to be performed in hippocampal neurons, preferably in a brain slice preparation. These future experiments should also be performed with single-molecule tracking techniques to ensure that true cluster dispersal is occurring as opposed to cluster fragmentation into domains below the resolution level of our current imaging approach.

At present, the mechanism(s) responsible for silencing clustered Kv2.1 channels is unknown. The Kv2.1 clusters are formed via a diffusion trap mechanism where mobile channels are retained behind a cytoskeletal corral (14). The simplest interpretation is that the mechanism responsible for this diffusion trap is also responsible for the nonconducting state. For example, we have postulated that the clustered Kv2.1 channels could be bound with retention proteins that sterically hinder the channel's ability to cross the cluster perimeter (14). These bound proteins could also effectively un-

couple S4 movement and pore opening. However, two completely distinct mechanisms could exist; e.g., bound proteins could still be responsible for the diffusion trap whereas channel phosphorylation or cluster-specific lipid content could control the potential for conductance. Future single-channel imaging experiments, in conjunction with voltage clamp, will be required to determine what percentage of the nonclustered channels are functional.

If the clustered channels do not become conducting, what is their purpose, especially in light of our Fig. 3 gating current data that suggest they still sense changes in membrane potential? The nonconducting roles of ion channels represent a unique area for ion channel biology that has begun to attract some attention (27). The clusters themselves must perform an important biological function in that they are regulated in hippocampal neurons by glutamate, hypoxia/ischemia, and G protein signaling, all of which elevate cytoplasmic Ca^{2+} (8, 9, 15). Most importantly, the clusters are located adjacent to glial cells and are regulated by astrocyte metabolism. For example, during ischemia, decreased glutamate uptake via the GLT-1 astrocyte glutamate transporter activates extrasynaptic neuronal NMDA receptors to initiate the Kv2.1 declustering (28, 29). The glial glutamate transporters, neuronal NMDA receptors, and Kv2.1 clusters are all localized adjacent to each other in hippocampal tissue. Such architecture and regulation likely exist for a reason.

One potential role of the Kv2.1 clusters is to communicate membrane potential to cytoplasmic signaling systems much like L-type Ca^{2+} channels link plasma membrane potential to cytoplasmic SR Ca^{2+} release in skeletal muscle (30). Another role for the Kv2.1 surface clusters involves membrane trafficking. Importantly, there is an expanding literature suggesting that Kv2.1 interacts with SNARE proteins and is involved in vesicle trafficking and/or fusion events (31). Perhaps the Kv2.1 clusters serve as sites where membrane potential modulates vesicular delivery to the surface or even vesicular release of neuro-active compounds.

In conclusion, our findings indicate that Kv2.1 surface clusters contain nonconducting channels whereas nonclustered channels provide the K^+ conductance underlying the recorded whole-cell currents. We propose that Kv2.1 clusters are not simply storage sites for nonconducting channels that are activated upon release from this cell surface microdomain. Whereas it is possible that more complex interventions are required to activate the clustered but silent channels, we favor the hypothesis that the Kv2.1 clusters represent cell surface structures crucial to cellular signaling pathways that are unrelated to ion conductance. Additional studies will determine whether the nonconducting Kv2.1 clusters are involved in Ca^{2+} signaling or membrane trafficking.

Materials and Methods

Molecular Biology, Cell Culture, Confocal Imaging, and General Electrophysiology. Details with respect to these methods are contained within *SI Text* and corresponding references (13, 14, 26, 32–36). Only low passage number (<45) HEK cells lacking endogenous K^+ channel activity were used. Channel number was estimated from ionic current using the equation $I = i \times P_o \times n$, where i is the single-channel current at +60 mV, P_o is the open probability, and n is channel number.

Single-Channel Measurements. Single-channel measurements for Kv2.1 were made using the cell-attached patch variant of the patch-clamp technique. To calculate the patch potential (V_{patch} = resting membrane potential – $V_{pipette}$), the cell's RMP was measured using the zero-current clamp method. Two methods were used that gave the same resting potential. In cells that were healthy at the end of a cell-attached patch-clamp experiment, the on-cell seal was ruptured and membrane potential measured in current clamp (with I clamped at 0). In this case, the measurement immediately after break-in was used, before significant diffusion of the pipette solution. A separate set of experiments was also performed to measure the RMP, using standard whole-cell pipette solutions. The average RMP was −74.9 ± 1.4 mV ($n = 10$), so −75 mV was used for all calculations of V_{patch}. All patches were held at the RMP ($V_{pipette} = 0$). Each on-cluster patch was depolarized to the test potential for 400 ms, with 400-ms intervals between depolarizations. Typically 50–100 sweeps were performed at each potential. Null sweeps (those with

no channel openings) were averaged and then subtracted from the sweeps with channel activity to obtain the ensemble average. Analysis of single-channel openings was done using the Single-Channel Search algorithm in Clampfit10. Mean single-channel current amplitudes were determined from a Gaussian fit of the all-points current histograms. The voltage dependence of the single-channel activity was estimated using ramp depolarizations from the RMP to +125 mV at a rate of 0.05 mV/ms. The single-channel current was estimated from the single-channel conductance using $i = g \times (V - E_K)$. For off-cluster patches, each patch was depolarized to +60 mV from the RMP in +10-mV increments using 200-ms test pulses. The peak I_K was plotted as a function of voltage and analyzed as described for whole-cell ionic currents. For additional details, see *SI Text*.

Whole-Cell Gating Current Measurements. Immobilization-resistant charge movements (gating currents) were measured by using TEA to block K+ currents through Kv2.1. The external recording solution contained 130 mM TEA-Cl, 5 mM KCl, 10 mM CaCl₂, 10 mM glucose, and 10 mM Hepes, pH 7.4. The internal (pipette) solution contained 140 mM NMDG-Cl, 1 mM MgCl₂, 4 mM NaCl, 0.5 mM EGTA, and 10 mM Hepes, pH 7.4. Gating currents were measured only from cells in which there was complete block of the ionic current. For additional details, see *SI Text*.

Declustering Experiments. For the simultaneous declustering, imaging, and whole-cell voltage-clamp analysis, cells containing clusters were first imaged followed by the establishment of the whole-cell voltage clamp configuration. After several minutes currents were recorded by stepping from a holding potential of −80 mV to test potentials of +60 to −70 mV, in 10-mV increments, 250 ms each. Following the test potential tail currents were recorded at −40 mV for 100 ms. Current properties from these early recordings were compared with those observed 15–25 min later after obvious declustering had occurred due to the addition of 200 nM swinholide A to the bath or the inclusion of alkaline phosphatase (500 units/mL) in the pipette. Alkaline phosphatase (molecular biology grade) was dialyzed against the intracellular pipette solution before use as previously described (15). Control cells voltage clamped for 15–25 min without actin depolymerization or alkaline phosphatase treatment showed a 1.34 ± 0.22-fold increase in current density and a 1.1 ± 1.9 mV depolarizing voltage shift in activation midpoint, $n = 11$. Three of these cells showed some declustering during the whole-cell recording.

1. Nerbonne JM (2000) Molecular basis of functional voltage-gated K+ channel diversity in the mammalian myocardium. *J Physiol* 525:285–298.
2. Misonou H, Trimmer JS (2004) Determinants of voltage-gated potassium channel surface expression and localization in mammalian neurons. *Crit Rev Biochem Mol Biol* 39:125–145.
3. Du J, Haak LL, Phillips-Tansey E, Russell JT, McBain CJ (2000) Frequency-dependent regulation of rat hippocampal somato-dendritic excitability by the K+ channel subunit Kv2.1. *J Physiol* 522:19–31.
4. Tamarina NA, Kuznetsov A, Fridlyand LE, Philipson LH (2005) Delayed-rectifier (KV2.1) regulation of pancreatic beta-cell calcium responses to glucose: Inhibitor specificity and modeling. *Am J Physiol Endocrinol Metab* 289:E578–E585.
5. Murakoshi H, Trimmer JS (1999) Identification of the Kv2.1 K+ channel as a major component of the delayed rectifier K+ current in rat hippocampal neurons. *J Neurosci* 19:1728–1735.
6. Mohapatra DP, et al. (2009) Regulation of intrinsic excitability in hippocampal neurons by activity-dependent modulation of the KV2.1 potassium channel. *Channels (Austin)* 3:46–56.
7. Malin SA, Nerbonne JM (2002) Delayed rectifier K+ currents, IK, are encoded by Kv2 alpha-subunits and regulate tonic firing in mammalian sympathetic neurons. *J Neurosci* 22:10094–10105.
8. Misonou H, et al. (2004) Regulation of ion channel localization and phosphorylation by neuronal activity. *Nat Neurosci* 7:711–718.
9. Misonou H, Mohapatra DP, Menegola M, Trimmer JS (2005) Calcium- and metabolic state-dependent modulation of the voltage-dependent Kv2.1 channel regulates neuronal excitability in response to ischemia. *J Neurosci* 25:11184–11193.
10. Misonou H, et al. (2006) Bidirectional activity-dependent regulation of neuronal ion channel phosphorylation. *J Neurosci* 26:13505–13514.
11. Pal SK, Takimoto K, Aizenman E, Levitan ES (2006) Apoptotic surface delivery of K+ channels. *Cell Death Differ* 13:661–667.
12. Lim ST, Antonucci DE, Scannevin RH, Trimmer JS (2000) A novel targeting signal for proximal clustering of the Kv2.1 K+ channel in hippocampal neurons. *Neuron* 25:385–397.
13. O'Connell KM, Rolig AS, Whitesell JD, Tamkun MM (2006) Kv2.1 potassium channels are retained within dynamic cell surface microdomains that are defined by a perimeter fence. *J Neurosci* 26:9609–9618.
14. Tamkun MM, O'connell KM, Rolig AS (2007) A cytoskeletal-based perimeter fence selectively corrals a sub-population of cell surface Kv2.1 channels. *J Cell Sci* 120:2413–2423.
15. Mohapatra DP, Trimmer JS (2006) The Kv2.1 C terminus can autonomously transfer Kv2.1-like phosphorylation-dependent localization, voltage-dependent gating, and muscarinic modulation to diverse Kv channels. *J Neurosci* 26:685–695.
16. Benndorf K, Koopmann R, Lorra C, Pongs O (1994) Gating and conductance properties of a human delayed rectifier K+ channel expressed in frog oocytes. *J Physiol* 477:1–14.
17. Trapani JG, Andalib P, Consiglio JF, Korn SJ (2006) Control of single channel conductance in the outer vestibule of the Kv2.1 potassium channel. *J Gen Physiol* 128:231–246.
18. Chapman ML, Krovetz HS, VanDongen AM (2001) GYGD pore motifs in neighbouring potassium channel subunits interact to determine ion selectivity. *J Physiol* 530:21–33.
19. Islas LD, Sigworth FJ (1999) Voltage sensitivity and gating charge in Shaker and Shab family potassium channels. *J Gen Physiol* 114:723–742.
20. Armstrong CM, Bezanilla F (1974) Charge movement associated with the opening and closing of the activation gates of the Na channels. *J Gen Physiol* 63:533–552.
21. Adams BA, Tanabe T, Mikami A, Numa S, Beam KG (1990) Intramembrane charge movement restored in dysgenic skeletal muscle by injection of dihydropyridine receptor cDNAs. *Nature* 346:569–572.
22. Stefani E, Toro L, Perozo E, Bezanilla F (1994) Gating of Shaker K+ channels: I. Ionic and gating currents. *Biophys J* 66:996–1010.
23. Park KS, Mohapatra DP, Misonou H, Trimmer JS (2006) Graded regulation of the Kv2.1 potassium channel by variable phosphorylation. *Science* 313:976–979.
24. Surmeier DJ, Foehring R (2004) A mechanism for homeostatic plasticity. *Nat Neurosci* 7:691–692.
25. Pal S, Hartnett KA, Nerbonne JM, Levitan ES, Aizenman E (2003) Mediation of neuronal apoptosis by Kv2.1-encoded potassium channels. *J Neurosci* 23:4798–4802.
26. Hulme JT, Coppock EA, Felipe A, Martens JR, Tamkun MM (1999) Oxygen sensitivity of cloned voltage-gated K(+) channels expressed in the pulmonary vasculature. *Circ Res* 85:489–497.
27. Kaczmarek LK (2006) Non-conducting functions of voltage-gated ion channels. *Nat Rev Neurosci* 7:761–771.
28. Misonou H, Thompson SM, Cai X (2008) Dynamic regulation of the Kv2.1 voltage-gated potassium channel during brain ischemia through neuroglial interaction. *J Neurosci* 28:8529–8538.
29. Mulholland PJ, et al. (2008) Glutamate transporters regulate extrasynaptic NMDA receptor modulation of Kv2.1 potassium channels. *J Neurosci* 28:8801–8809.
30. Tanabe T, Beam KG, Powell JA, Numa S (1988) Restoration of excitation-contraction coupling and slow calcium current in dysgenic muscle by dihydropyridine receptor complementary DNA. *Nature* 336:134–139.
31. Feinshreiber L, Singer-Lahat D, Ashery U, Lotan I (2009) Voltage-gated potassium channel as a facilitator of exocytosis. *Ann N Y Acad Sci* 1152:87–92.
32. Kwak YG, Navarro-Polanco RA, Grobaski T, Gallagher DJ, Tamkun MM (1999) Phosphorylation is required for alteration of kv1.5 K(+) channel function by the Kvbeta1.3 subunit. *J Biol Chem* 274:25355–25361.
33. Martens JR, et al. (2000) Differential targeting of Shaker-like potassium channels to lipid rafts. *J Biol Chem* 275:7443–7446.
34. Martens JR, Sakamoto N, Sullivan SA, Grobaski TD, Tamkun MM (2001) Isoform-specific localization of voltage-gated K+ channels to distinct lipid raft populations. Targeting of Kv1.5 to caveolae. *J Biol Chem* 276:8409–8414.
35. O'Connell KM, Tamkun MM (2005) Targeting of voltage-gated potassium channel isoforms to distinct cell surface microdomains. *J Cell Sci* 118:2155–2166.
36. O'Connell KM, Whitesell JD, Tamkun MM (2008) Localization and mobility of the delayed-rectifer K+ channel Kv2.1 in adult cardiomyocytes. *Am J Physiol Heart Circ Physiol* 294:H229–H237.